International Journal of Thermophysics, Vol. 18, No. 1, 1997

Experimental Investigation of Nonuniform Heating and Heat Loss from a Specimen for the Measurement of Thermal Diffusivity by the Laser Pulse Heating Method

T. Yamane,[1,2] S. Katayama,[1] and M. Todoki[1]

Received April 22, 1996

Nonuniform heating effect and heat loss effect from the specimen in the measurement of thermal diffusivity by the laser pulse heating method have been experimentally investigated using an axially symmetric Gaussian laser beam and a laser beam homogenized with an optical filter. The degree of error is theoretically estimated based on the solution of the two-dimensional heat conduction equation under the boundary condition of heat loss from the surface of the specimen in the axial direction and the initial conditions of axially symmetric nonuniform and uniform heating. A correction factor, which is determined by comparison of the entire experimental and the theoretical history curves, is introduced to correct the values obtained by the conventional $t_{1/2}$ method. The applicability of this modified curve-fitting method has been experimentally tested using materials in the thermal diffusivity range 10^{-3} to 1 $cm^2 \cdot s^{-1}$. The experimental error due to the nonuniform heating and heat loss was reduced to approximately 3%.

KEY WORDS: laser pulse heating method; nonuniform heating; thermal diffusivity.

1. INTRODUCTION

The laser pulse heating method for measuring thermal diffusivity was developed by Parker et al. [1] in 1961 using the analytical solution for one-dimensional heat flow under the following conditions.

[1] Materials Characterization Laboratories, Toray Research Center, Inc., Sonoyama 3-3-7, Otsu, Shiga 520, Japan.

[2] To whom correspondence should be addressed.

0195-928X/97/0100-0269$12.50/0

(a) The duration of the laser pulse is negligibly short compared to the characteristic time of thermal diffusion.

(b) The front surface of the specimen is uniformly heated by a spatially homogenized laser beam.

(c) The specimen is adiabatic during measurement after the laser energy is absorbed.

(d) The specimen is uniform (in geometry) and homogeneous.

(e) The specimen is nontransparent to the laser beam and to thermal radiation.

The thermal diffusivity, α, is calculated from the measured time–temperature curve of the back surface of the specimen based on the "$t_{1/2}$ method" using

$$\alpha = 1.370 \frac{b^2}{\pi^2 t_{1/2}} \tag{1}$$

where b is the thickness of the specimen and $t_{1/2}$ is the half-rise time defined by the interval required for the back-surface temperature to reach one-half of the maximum temperature rise. Currently, the laser pulse heating method is generally accepted as the standard method for measuring the thermal diffusivity of solid materials [2]. However, some of the above conditions, particularly conditions (a) and (b), are not entirely satisfied in the actual measurements. For condition (a), the finite duration of the laser pulse effect can be corrected by Azumi and Takahashi's [3] center-of-gravity of the pulse method. For condition (b), radiative heat loss from the specimen surface is unavoidable, especially in high-temperature experiments. Some algorithms which take the radiative heat loss into consideration have been theoretically developed by, for example, Cowen [4], Cape and Lehman [5], Heckmann [6], and Clark and Taylor [7]. Cape and Lechman's paper has been referenced quite extensively [8–11] as a correction to the theory developed by Parker et al. They account for radiative heat loss by replacing the factor 1.370 in Parker's relationship Eq. (1) by a function of the Biot number. These authors did not consider nonuniform heating, i.e., condition (c), and recently it was pointed out that Cape and Lechman had made a mathematical error in their analysis [12]. For condition (c), analytical calculation of nonuniform heating has been made by Watt [13] and McKay and Schriempf [14]. Based on their solution, the nonuniform heating error for specimens of various dimensions has been calculated under various energy distributions of heating by Azumi et al. [15] and Baba et al. [16, 17]. Recently, Cezairliyan et al. [18] have

developed a new system for accurate measurements of thermal diffusivity. In their data analysis, the entire region of the temperature history curve is fitted to Cape and Lehman's theoretical solution to correct for the radiative heat loss. They called this procedure the "curve-fitting method." The particular advantage of the curve-fitting method over other methods is that the quality of experimental data can be checked by observing the discrepancy between the experimental and the theoretical curve. As mentioned above, some investigators have theoretically estimated nonuniform heating with heat loss from the specimen, but this is not yet experimentally confirmed. We have experimentally confirmed the degree of error resulting from nonuniform heating using an axially symmetric Gaussian laser beam, and developed a modified curve-fitting method to correct for nonuniform heating and heat loss from the specimen simply using the solution by Watt [13].

2. THEORY

Figure 1 shows the schematic diagram of the geometry for the pulse heating method which takes nonuniform heating and radiative heat losses into consideration, where a is the sample radius and b is the sample thickness. The heat conduction equation is

$$\frac{\partial^2 T(x, r, t)}{\partial r^2} + \frac{1}{r}\frac{\partial T(x, r, t)}{\partial r} + \frac{\partial^2 T(x, r, t)}{\partial x^2} + \frac{Q(x, r, t)}{\alpha C} - \frac{1}{\alpha}\frac{\partial T(x, r, t)}{\partial t} = 0 \qquad (2)$$

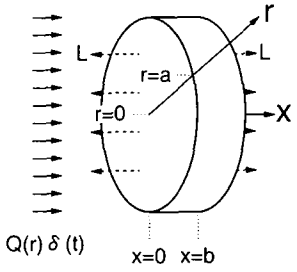

Fig. 1. A schematic diagram of the geometry for the pulse heating method. The energy $Q(r)$ is instantaneously supplied to the front surface of the specimen ($x=0$) at time 0. There is some radiative heat loss from the front and back surfaces of the specimen.

where $Q(x, r, t)$ is the energy absorbed by the specimen, C is the heat capacity of the specimen, and α is the thermal diffusivity of the specimen. If there is radiative heat loss from the front and back surfaces, the boundary condition can be approximated by

$$-\frac{\partial T(x, r, t)}{\partial x}+\frac{L}{b} T(x, r, t)=0 \qquad \text{at} \quad x=0 \tag{3}$$

$$\frac{\partial T(x, r, t)}{\partial x}+\frac{L}{b} T(x, r, t)=0 \qquad \text{at} \quad x=b \tag{4}$$

where L is the radiative heat loss parameter, called the Biot number, and is defined as

$$L=\frac{4\varepsilon\sigma T^3 b}{\lambda} \tag{5}$$

where ε is the emissivity of the surface, σ is the Stefan–Boltzmann constant, T is the steady-state temperature of the specimen, and λ is the thermal conductivity of the specimen. Since the temperature difference between the surface of the specimen and the environment is small for the pulse heating method, the usual fourth-power law of radiation heat transfer may be approximated by the above linear relation [13]. The radiative heat loss in the radial direction may be neglected, since there is only a small gap between the cylindrical side of the specimen and the inside wall of the holder in the actual experiment, and it is estimated that the radiative heat loss from the side surface of the specimen is smaller than heat losses from the front and back surfaces of the specimen. The front surface of the specimen is subjected to pulsewise heating, i.e., the initial condition is

$$Q(x, r, t)=Q(r) \qquad \text{at} \quad t=0 \qquad \text{for} \quad x=0 \tag{6}$$

where $Q(r)$ is the energy absorbed at r, and the analytical solution of Eq. (2) is given by Watt [13] as the product of the component solutions,

$$T(x, r, t)=T_0 T_x(x, t)\, T_r(r, t) \tag{7}$$

where $T_0=Q_0/C$, the equilibrium temperature increase, $T_x(x, t)$ is the x component, $T_r(r, t)$ is the r component, and Q_0 is the total energy absorbed by the specimen. $T_x(x, t)$ is given by

$$T_x(x, t)=\sum_{n=1}^{\infty} Y_n(0)\, Y_n(x) \exp\left(-\frac{\beta_n^2 t}{\pi^2 t_c}\right) \tag{8}$$

where

$$Y_n(x') = \frac{\{2(\beta_n^2 + L^2)\}^{1/2} \{\beta_n \cos \beta_n(x'/b) + L \sin \beta_n(x'/b)\}}{\{(\beta_n^2 + L^2)(\beta_n^2 + L^2 + L) + L(\beta_n^2 + L^2)\}^{1/2}} \tag{9}$$

β_n ($n = 1, 2, 3,...$) are positive roots of

$$\tan \beta_n = \frac{2\beta_n L}{\beta_n^2 - L^2} \tag{10}$$

and t_c is the characteristic time defined by

$$t_c = \frac{b^2}{\pi^2 \alpha} \tag{11}$$

Equations (8)–(11) show that the nondimensional time, t/t_c, dependence of $T_x(x, t)$ is a function of x and L. $T_r(r, t)$ is given by

$$T_r(r, t) = \frac{2}{a^2} \left\{ \int_0^a rg(r)\, dr + \sum_{i=1}^{\infty} \frac{J_0(Z_i r/a)}{J_0(Z_i)} \exp\left(-Z_i^2 \frac{b^2 t}{\pi^2 a^2 t_c} \right) \times \int_0^a rg(r)\, J_0(Z_i r/a)\, dr \right\} \tag{12}$$

where $g(r)$ is the axially symmetric energy distribution absorbed by the specimen surface, J_0 is the Bessel function of the first kind of order 0, and Z_i ($i = 1, 2, 3,...$) are positive roots of

$$J_1(Z_i) = 0 \tag{13}$$

where J_1 is the Bessel function of the first kind of order 1. In Eqs. (12)–(13) the definite integral term with respect to r can be integrated numerically or analytically, and is independent of t/t_c, if the shape of $g(r)$ in the region from $r = 0$ to $r = a$ is determined experimentally. In this integration $g(r)$ need only be axially symmetric. Equations (12) and (13) show that the nondimensional time, t/t_c, dependence of $T_r(x, t)$ is a function of r and the ratio of thickness to radius b/a, if $g(r)$ is axially symmetric.

In the actual experiment, a radiation detector which detects the average temperature of the region of interest is often used as the temperature detector. From Eq. (7), the back surface temperature response, $T_{cal}(b/a, L, t)$, which is within a circle located at the center of the specimen, can be estimated by

$$T_{cal}(b/a, L, t) = T_0 T_x(b, t) \int_0^{r_{obs}} \frac{2r}{r_{obs}^2} T_r(r, t)\, dr \tag{14}$$

where r_{obs} is the radius of the detected area, b/a is the shape parameter related to $T_r(r, t)$ and L is the heat loss parameter related to $T_x(x, t)$. If the specimen surface is uniformly heated, i.e., $g(r) = 1$, then $T_r(r, t) = 1$, and $T_{cal}(b/a, L, t)$ is represented as

$$T_{cal}(b/a, L, t) = T_0 T_x(b, t) \tag{15}$$

which is independent of b/a. In the following discussion, the shape parameter, b/a is considered 0 for the uniform heating. If there is no heat loss from the specimen, i.e., $L = 0$, $T_x(b, t)$ is given by

$$T_x(b, t) = 1 + 2 \sum_{n=1}^{\infty} (-1)^n \exp\left(-\frac{n^2 t}{\pi^2 t_c}\right) \tag{16}$$

Substituting Eq. (16) into Eq. (15), we obtain the analytical solution based on the conventional $t_{1/2}$ method [1]. If the specimen surface is uniformly heated, i.e., $b/a = 0$, and there is no heat loss from the specimen, i.e., $L = 0$, the time, $t_{1/2}(0, 0)$, at which the calculated temperature response, $T_{cal}(0, 0, t)$, reaches $T_0/2$ is

$$t_{1/2}(0, 0) = 1.370 t_c \tag{17}$$

which is the conventional $t_{1/2}$ result given in Eq. (1).

3. APPARATUS

The experiments were performed using a commercially available apparatus (Shinku-Riko Inc., Type TC-7000) for the thermal diffusivity measurements. A ruby laser is used for pulse heating the specimen. The irradiated area is a circle about 12 mm in diameter, the maximum energy per pulse is 7 J, and the pulse duration is about 3 ms. The optical center of a ruby laser and the specimen are aligned based on the energy distribution absorbed by the specimen's surface which is experimentally determined (see Section 5). Time 0 was set at the center of gravity of the laser pulse energy on the time scale to correct for the finite pulse effect [3]. A handmade optical reduction filter is used to improve the spatial energy distribution of the ruby laser. The optical filter is an approximately $1.5 \times 3 \times 3\text{-mm}^3$ rectangular solid made of acrylic resin and cuts out 70% of the energy of the laser incident on the surface. The optical filter is placed on the optical axis outside the furnace part. An InSb infrared radiation detector is used as the temperature detector; its response time is about 5 μs. The tantalum slit is placed between the specimen and the detector to avoid direct irradiation of the detector by the ruby laser. The slit has a 5-mm-diameter hole

through its center. The optical centers of the detector and the specimen are aligned using a guide beam system, which can be placed at the center of the specimen's position. Using this system, the radius of the detected area on the specimen, r_{obs} in Eq. (14), is 2.5 mm, which is about half the specimen radius, i.e., $r_{obs} = a/2$. The electronically amplified analog signal is digitized and stored in a transient-wave memory with a capacity of 8 k words of 10 bits each. The data are then transferred to a personal computer for processing. A specimen is placed vertically in the specimen holder, and the specimen chamber is evacuated to about 10^{-3} Torr using a rotary pump. The specimen and the specimen holder make only pinpoint contact, thus heat conduction between them can be neglected.

4. SPECIMEN

Our procedure has been developed and applied to the measurement of the four specimens shown in Table I. The specimen diameter is 10 mm for all materials. Specimens of various thicknesses are prepared in order to check the effect of nonuniform heating. Dry graphite carbon is sprayed on the front surface to absorb the energy of the beam and on the back surface to increase the emissivity.

5. EXPERIMENTS

The distribution of energy absorbed by the specimen surface, $g(r)$, must be determined to calculate the temperature–response curve using Eq. (14). We experimentally determined $g(r)$ according to the following steps.

(a) A dry graphite/carbon-sprayed copper of cubic block about $1 \times 1 \times 1$ mm^3 is attached to a platinum platinum–rhodium thermocouple wire of 0.1-mm diameter.

(b) The cubic block is placed the position of the center of the specimen in the present system without the specimen.

(c) The ruby laser is irradiated and the time dependence of the temperature rise of the copper block is determined.

(d) The cooling part of the observed curve is least-squares fitted to the exponential curve.

(e) The exponential curve is extrapolated to Time 0 and $T_{max}(0)$ is determined.

(f) The copper block is shifted to a position at a distance r away from the center of the sample in the horizontal or vertical direction.

Table I. Properties of Samples

Sample	Chemical composition	Sample thickness at 298.15 K, h (mm)	Thermal diffusivity from other sources at 298.15 K, α ($cm^2 \cdot s^{-1}$)	Remarks
Aluminum	Purity, 99.99 mol%	1.486, 1.963, 2.454, 3.016	0.968[a]	
Molybdenum	Purity, 99.99 mol%	1.011, 1.542, 2.031, 2.542, 3.036	0.543[a]	
Alumina	$Al_2O_3 > 99.7$ wt%	1.003, 1.507, 2.008, 2.501	0.101[b]	Density, 3.92 $g \cdot cm^{-3}$; fine ceramic supplied by Japan Fine Ceramics Center
MACOR	SiO_2, 46 wt%; MgO, 17 wt%; Al_2O_3, 16 wt%; K_2O, 10 wt%; B_2O_3, 7 wt%; F, 4 wt%	0.534, 1.019, 1.516, 2.034, 2.486	0.009[c]	Machinable ceramic supplied by Corning Inc.

[a] See Ref. 19.
[b] See Ref. 20.
[c] See MACOR Technical Report supplied by Corning Inc.

(g) $T_{max}(r)$ is determined in the same manner as steps (b)–(d).

(h) In the region $-1.5a < r < 1.5a$, steps (b)–(f) are repeated.

(i) The energy distribution is estimated using

$$g(r) = \frac{T_{max}(r)}{T_{max}(0)} \tag{18}$$

Figure 2 shows the distribution of energy absorbed by the specimen surface irradiated directly by the ruby laser. The center of the specimen surface is intensely heated. The dashed line in Fig. 2 shows the values calculated using

$$g(r) = \exp\left(-\frac{r^2}{0.25}\right) \tag{19}$$

assuming a Gaussian distribution. We call this nonuniform heating and calculate the temperature response using Eq. (19). We attempted to improve the uniformity of the energy absorbed by the specimen surface by reducing the intensity of the laser around the center using an optical reduction filter. Figure 3 shows the distribution of energy absorbed by the specimen surface, when the nonuniform ruby laser shown in Fig. 2 is irradiated through a handmade optical reduction filter. Figure 3 shows that in the region, $-a < r < a$ the specimen surface is more uniformly heated.

Figure 4 shows an example of the theoretical curve for the nonuniform heating calculated using Eq. (14) with Eq. (19) under the conditions of

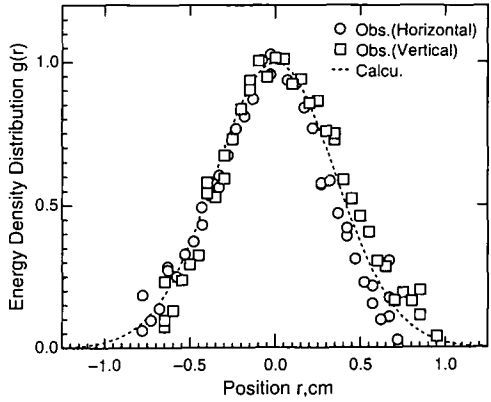

Fig. 2. Energy distribution of the ruby laser used in this work. The dashed line shows the curve calculated using Eq. (19).

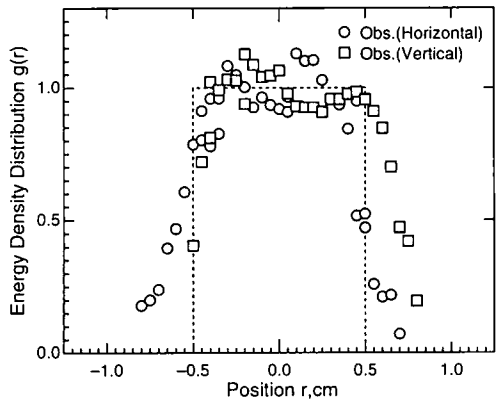

Fig. 3. Energy distribution of the ruby laser used in this work homogenized with a handmade optical reduction filter.

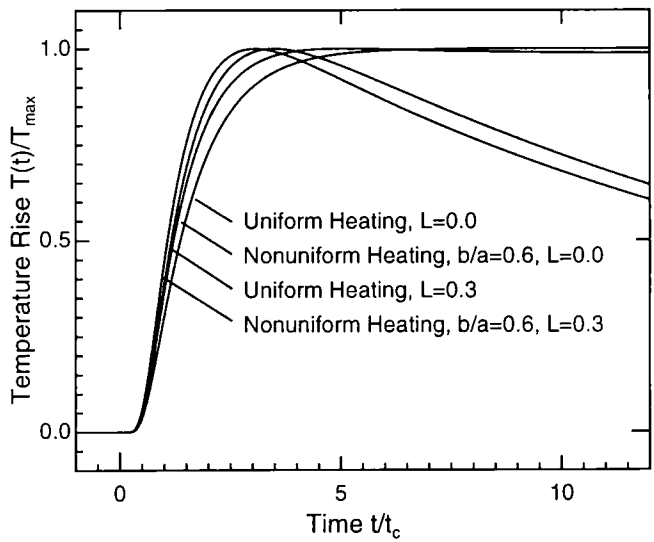

Fig. 4. Example of the theoretical curve for the nonuniform heating calculated using Eq. (14) with Eq. (19) under the conditions of radius of the detected area $r_{obs} = a/2$, shape parameter $b/a = 0.6$ and the heat loss parameter $L = 0.0$ and 0.3, and an example of the theoretical curve for the uniform heating calculated using Eq. (15) under the conditions of heat loss parameter $L = 0.0$ and 0.3.

radius of the detected area $r_{obs} = a/2$, shape parameter $b/a = 0.6$, and heat loss parameter $L = 0.0$ and 0.3, and an example of the theoretical curve for uniform heating calculated using Eq. (15) under the conditions of $L = 0.0$ and 0.3. Figure 4 shows that the half-time $t_{1/2}/t_c$ for axially symmetric Gaussian nonuniform heating, as shown in Fig. 2 or Eq. (19), is shorter than that of the conventional method, i.e., $t_{1/2}(b/a, L)/t_c = 1.217$ for $b/a = 0.6$ and $L = 0.0$. Figure 4 show that the half-time $t_{1/2}/t_c$ for both nonuniform and uniform heating becomes short as the heat loss effect becomes large, i.e., $t_{1/2}(b/a, L)/t_c = 1.076$ for $b/a = 0.6$ and $L = 0.3$ under nonuniform heating conditions, and $t_{1/2}(b/a, L)/t_c = 1.165$ for $L = 0.3$ under uniform heating conditions. This estimation agrees with the other reported theoretical considerations [4–7, 13–17]. Figure 4 shows that the time dependence of the back surface under the conditions of axially symmetric Gaussian nonuniform heating without any heat loss from the specimen is apparently the same as that under the conditions of uniform heating with heat loss from the specimen. This resemblance of the temperature history curve for axially symmetric Gaussian nonuniform heating and heat loss effect leads to the risk of misinterpreting the axially symmetric Gaussian nonuniform heating effect as the heat loss effect, if the distribution of energy absorbed by the specimen has not been confirmed. It is concluded that in the actual experiment the distribution of energy absorbed by the specimen must be checked in order to apply the theoretically derived correction method to correct for the heat loss effect, which does not take account of the nonuniform heating effect.

To correct for the nonuniform heating and heat loss effect estimated above, we introduce the correction factor

$$K(b/a, L) = \frac{t_{1/2}(b/a, L)}{t_{1/2}(0, 0)} = \frac{t_{1/2}(b/a, L)}{1.370 t_c} \tag{20}$$

The correction factor $K(b/a, L)$ replaces the factor 1.370 in Parker's relationship Eq. (1) by a function of b/a and L. Using this factor, thermal diffusivity can be determined using

$$\alpha = \alpha^* K(b/a, L) \tag{21}$$

where α^* is the apparent thermal diffusivity derived from the observed curve using

$$\alpha^* = 1.370 \frac{b^2}{\pi^2 t_{1/2}} \tag{22}$$

which is that of the conventional $t_{1/2}$ method.

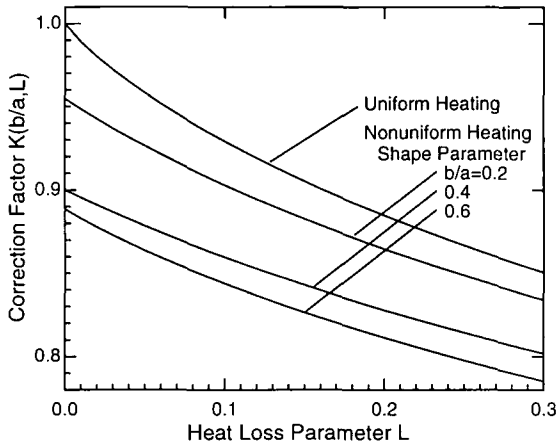

Fig. 5. Heat loss parameter dependence of the correction factor $K(b/a, L)$.

Figure 5 shows how the correction factor depends on b/a and L for nonuniform heating from Eq. (14) and L for uniform heating from Eq. (15). From Fig. 5, it is clear that the thermal diffusivity obtained by the conventional $t_{1/2}$ method is 11% smaller than the true value for axially symmetric Gaussian nonuniform heating, $b/a = 0.4$, absent heat loss. Although the shape parameter, b/a, can be determined easily from the dimensions of the specimen, the heat loss parameter, L, must be determined from the comparison of observed and theoretical normalized time dependence curves by the following steps.

(a) The time axis of the observed temperature rise $T_{obs}(t)$ is normalized so that $t_{1/2}/t_c^* = 1.370$, where t_c^* is the apparent characteristic time defined as

$$t_c^* = \frac{b^2}{\pi^2 \alpha^*} \tag{23}$$

where α^* is the apparent thermal diffusivity obtained from Eq. (22).

(b) The object function defined as

$$F(b/a, L) = \frac{\sqrt{\sum_{i=1}^{n} \{T_{obs}(t_i/t_c^*)/T_{max} - T_{cal}(b/a, L, t_i/t_c^*)/T_{max}\}^2}}{n} \tag{24}$$

is calculated, where $T_{cal}(b/a, L, t/t_c^*)/T_{max}$ is the calculated curve, the time axis normalized so that $t_{1/2}(b/a, L)/t_c^* = 1.370$.

(c) The heat loss parameter dependence of $F(b/a, L)$ is calculated.

(d) The curve which has minimum $F(b/a, L)$ is adopted as the best-fit curve.

Figure 6 shows examples of the theoretical curves, the time axis normalized so that $t_{1/2}(b/a, L)/t_c^* = 1.370$, for nonuniform heating and uniform heating, of which original time dependence is shown in Fig. 4.

A time normalization technique using $t_{1/2}$ similar to the present method has been utilized by other researchers to correct for heat loss. Clark and Taylor [7] used a few points of the heating part of these curves and Cowan [4] used a few points of the cooling part of these curves. In contrast to these methods, the present method uses the entire curve in Eq. (24). This method is superior to the other methods for the following reasons, as for the curve-fitting method [18].

(a) The other methods may be more sensitive to experimental noise than the present method when determing the correction factor.

(b) When using the present method, the quality of the experimental data can be checked by observing the discrepancy between the experimental and the theoretical curves.

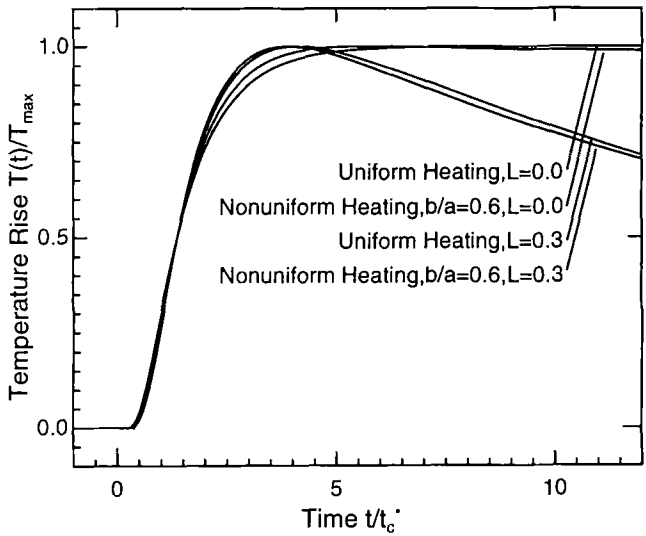

Fig. 6. Example of the theoretical curve, the time axis normalized so that $t_{1/2}(b/a, L)/t_c^* = 1.370$, for nonuniform heating and uniform heating, of which the original time dependence is shown in Fig. 4.

As for reason (b), in the actual experiment, if the discrepancy between the observed and the theoretical curves becomes large, we must check the experimental conditions, e.g., the energy distribution absorbed by the specimen surface. We call the present procedure the modified curve-fitting method to account for the nonuniform heating.

Figure 7 shows a typical example of the observed data, time axis normalized so that $t_{1/2}(b/a, L)/t_c^* = 1.370$, for molybdenum (2.542 mm in thickness at 298.15 K) under the nonuniform heating condition at 298.15 K. The apparent thermal diffusivity $\alpha^* = 0.631\ \mathrm{cm^2 \cdot s^{-1}}$, and the apparent characteristic time $t_c^* = 10.37$ ms. The dashed line shows the theoretical curve calculated using Eq. (14) with Eq. (19) for $b/a = 0.5$ and

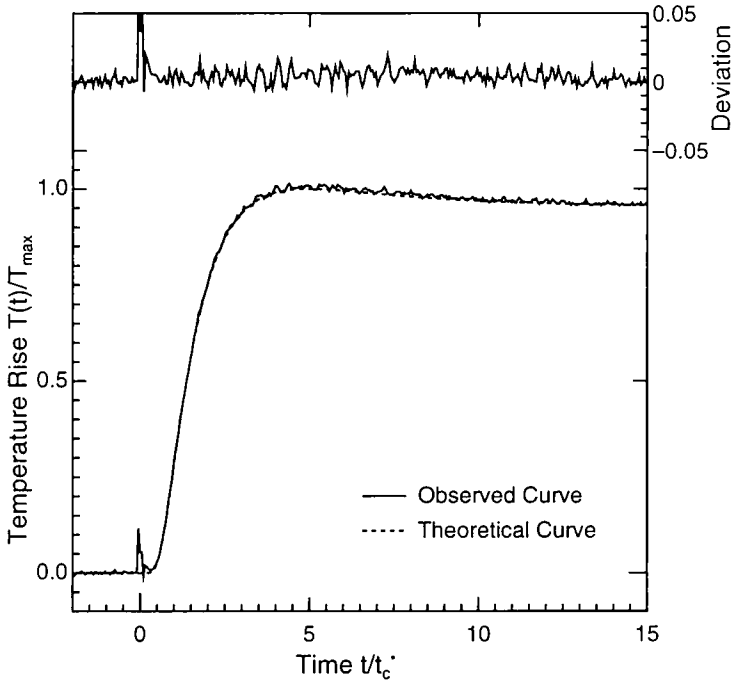

Fig. 7. Example of the observed curve, the time axis normalized so that $t_{1/2}(b/a, L)/t_c^* = 1.370$, for molybdenum (2.542 mm in thickness at 298.15 K) under nonuniform heating conditions at 298.15 K. The dashed line is the theoretical curve, the time axis normalized so that $t_{1/2}(b/a, L)/t_c^* = 1.370$, using Eq. (14) with Eq. (19) for shape parameter $b/a = 0.5$ and heat loss parameter $L = 0.0$. The apparent thermal diffusivity α^* obtained by the conventional $t_{1/2}$ method is $0.631\ \mathrm{cm^2 \cdot s^{-1}}$, the apparent characteristic time t_c^* is 10.37 ms, and the corrected thermal diffusivity α obtained by the present modified curve-fitting method is $0.560\ \mathrm{cm^2 \cdot s^{-1}}$.

$L = 0.0$, time axis is normalized so that $t_{1/2}(b/a, L)/t_c^* = 1.370$. Since, under the above condition, the correction factor $K(b/a, L) = 0.8877$, the true thermal diffusivity a equals $0.560\ \mathrm{cm}^2 \cdot \mathrm{s}^{-1}$. The quality of the measurement can be judged by the fit between the observed and the theoretical curve. This result shows that Eq. (14) with Eq. (19) accurately represents the time dependence of the temperature rise of the back surface under the nonuniform heating conditions and thus the correction factor $K(b/a, L)$ should correct for the nonuniform heating.

Figure 8 shows a typical example of the observed data, time axis normalized so that $t_{1/2}(b/a, L)/t_c^* = 1.370$, for the same specimen as shown in Fig. 7 with uniform heating at 298.15 K. The difference in the shapes of the observed temperature rise curves in Fig. 7 and Fig. 8 reflects the difference in the spatial distribution of energy absorbed by the specimen surface. The

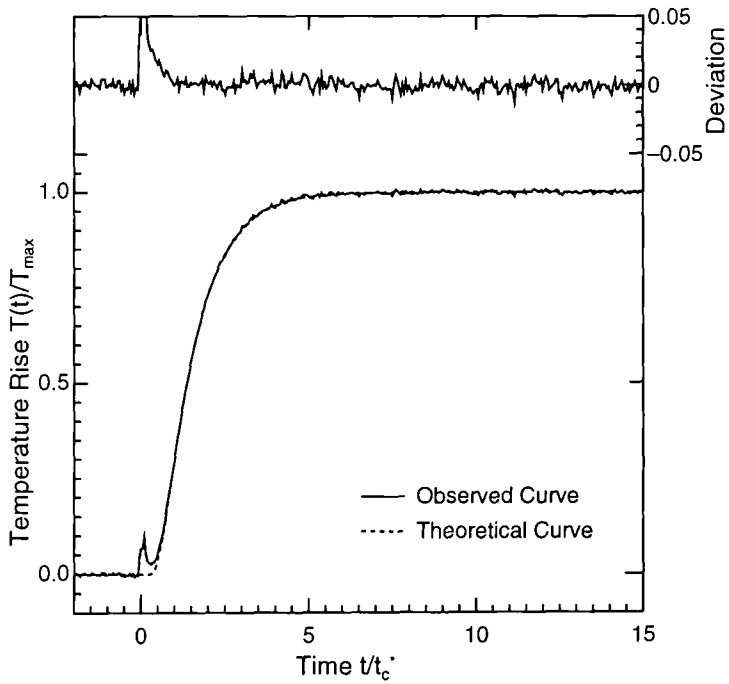

Fig. 8. Example of the observed curve, the time axis normalized so that $t_{1/2}(b/a, L)/t_c^* = 1.370$, for the same molybdenum specimen as shown in Fig. 7 under uniform heating at 298.15 K. The dashed line is the theoretical curve, the time axis normalized so that $t_{1/2}(b/a, L)/t_c^* = 1.370$, calculated using Eq. (15) for heat loss parameter $L = 0.0$, i.e., Eq. (16). The apparent thermal diffusivity α^* obtained by the conventional $t_{1/2}$ method is $0.557\ \mathrm{cm}^2 \cdot \mathrm{s}^{-1}$, and the apparent characteristic time t_c^* is 11.76 ms. Under this condition, α^* and t_c^* equal α and t_c.

apparent thermal diffusivity $\alpha^* = 0.557\ \mathrm{cm}^2 \cdot \mathrm{s}^{-1}$, and the apparent characteristic time $t_c^* = 11.76$ ms. The dashed line shows the theoretical curve calculated using Eq. (15) for $L = 0.0$, i.e., Eq. (16), which corresponds to Parker's analytical solution. The observed curve agrees with the theoretical curve in this time range. It is concluded that under this condition, α^*, t_c^*, and $K(b/a, L) = \alpha$, t_c, and 1.0, respectively. This result shows that the improved ruby laser can be considered as a uniform heat source, and that an optical filter succeeds in reducing the nonuniformity of the laser.

Figure 9 shows a typical example of the observed data, time axis normalized so that $t_{1/2}(b/a, L)/t_c^* = 1.370$, for MACOR (2.486 mm in thickness at 298.15 K) under uniform heating conditions i.e., $b/a = 0$, with heat loss at 873.15 K. The apparent thermal diffusivity $\alpha^* = 6.59 \times 10^{-3}\ \mathrm{cm}^2 \cdot \mathrm{s}^{-1}$,

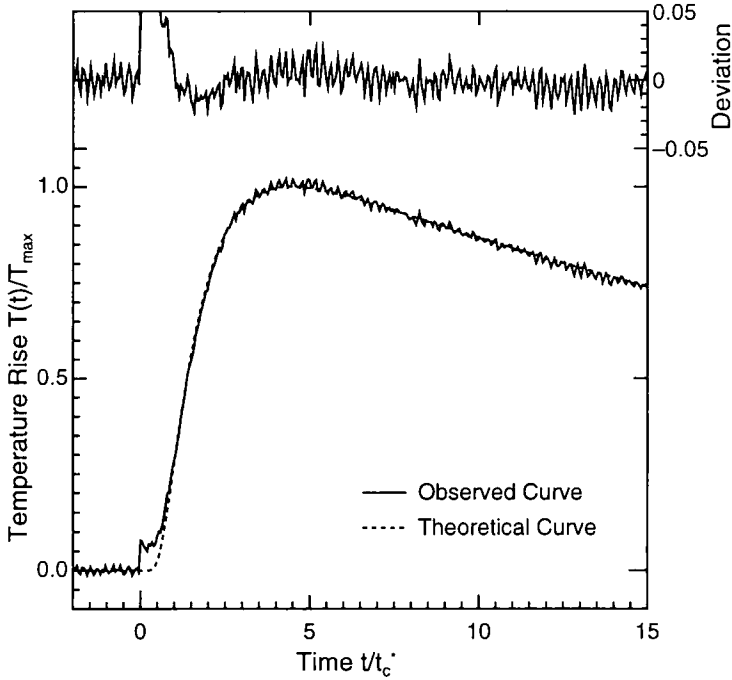

Fig. 9. Example of the observed curve, the time axis normalized so that $t_{1/2}(b/a, L)/t_c^* = 1.370$, for MACOR (2.486 mm in thickness at 298.15 K) under uniform heating with heat loss at 873.15 K. The dashed curve is the theoretical curve, the time axis normalized so that $t_{1/2}(b/a, L)/t_c^* = 1.370$, using Eq. (15) for heat loss parameter $L = 0.18$. The apparent thermal diffusivity α^* obtained by the conventional $t_{1/2}$ method is $6.59 \times 10^{-3}\ \mathrm{cm}^2 \cdot \mathrm{s}^{-1}$, the apparent characteristic time t_c^* is 1.302 s, and the corrected thermal diffusivity α obtained by the present modified curve-fitting method is $5.88 \times 10^{-3}\ \mathrm{cm}^2 \cdot \mathrm{s}^{-1}$.

and the apparent characteristic time $t_c^* = 1.302$ s. The heat loss parameter is determined by the present modified curve-fitting method. Figure 10 shows the relationship between the heat loss parameter L and the object function $F(b/a, L)$ [see Eq. (24)] for the curves shown in Fig. 9. The object function $F(b/a, L)$ is calculated under the following conditions.

Time step [$=(t_{j+1}/t_c^*)-(t_j/t_c^*)$]:	0.05
Time range:	$t_1/t_c^* = 0.05$, $t_n/t_c^* = 1.50$
Number of data points ($=n$):	300

Figure 10 shows that the theoretical curve for $L = 0.18$ gives the best match to the experimental curve. Since the correction factor $K(b/a, L)$ equals 0.8926 for $L = 0.18$, the true thermal diffusivity $\alpha = 5.88 \times 10^{-3}\ \mathrm{cm^2 \cdot s^{-1}}$. The dashed line in Fig. 9 shows the theoretical curve calculated using Eq. (15) for $L = 0.18$, time axis normalized so that $t_{1/2}(b/a, L)/t_c^* = 1.370$. This result shows that the present modified curve-fitting method accurately represents the time dependence of the temperature rise of the back surface with heat loss from the specimen, and thus the correction factor $K(b/a, L)$ should accurately correct for heat loss, similarly to the case of nonuniform

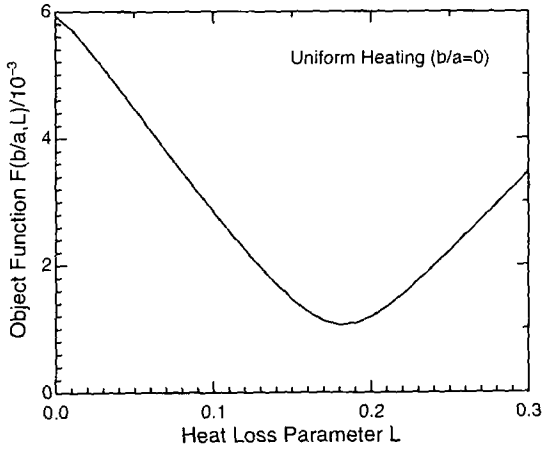

Fig. 10. Heat loss parameter dependence of the object function $F(b/a, L)$ for the data shown in Fig. 9. As the specimen surface is uniformly heated, the shape parameter, b/a, equals 0 according to our definition (for details, see, the text). The minimum at $L = 0.18$ determines the value of the Biot number L used to generate the dashed curve in Fig. 9.

heating. Table II lists thermal diffusivity values obtained by the present method compared with those calculated by commonly used methods to correct for heat loss under the uniform heating condition using the data shown in Fig. 9. There is essentially no difference between the thermal diffusivity values after heat loss correction, which is natural as all methods are based on the same theoretical formula. The particular advantage of the present method is that the quality of experimental data can be checked by observing the discrepancy between the experimental and the theoretical curve as shown in Fig. 9 using the object function as shown in Fig. 10.

Figure 11 shows the thermal diffusivity at 298.15 K obtained by the following three methods: (a) the conventional $t_{1/2}$ method under nonuniform heating conditions, (b) the present modified curve-fitting method under nonuniform heating conditions, and (c) the present modified curve-fitting method under the uniform heating conditions. For all the samples, as the shape parameter increases, the thermal diffusivity obtained by the conventional $t_{1/2}$ method under nonuniform heating condition increases. For aluminum and molybdenum, this tendency results from the axially symmetric Gaussian nonuniform heating effect, which has been theoretically estimated from $K(b/a, L)$ dependence on b/a and experimentally confirmed from the agreement between the shape of the entire observed temperature history curve and the theoretical curve without heat loss effect for all of these specimens as in Figs 7 and 8. For aluminum and molybdenum, thermal diffusivities obtained by the present modified curve-fitting method are independent of the shape parameter and energy distribution of the heating source and agree with the reported values [19] within 3%. For

Table II. Comparison Between the Thermal Diffusivity Values Corrected for Heat Loss Effect Based on Different Data Analysis Algorithms from the Temperature History Curve Shown in Fig. 9 Under Uniform Heating Conditions

Data analysis algorithms	Thermal diffusivity, α ($cm^2 \cdot s^{-1}$)
Present method	5.88×10^{-3}
Cowan [4]	
$T(5t_{1/2})/T(t_{1/2})$	5.83×10^{-3}
$T(10t_{1/2})/T(t_{1/2})$	5.83×10^{-3}
Clark and Taylor [7]	
$t_{0.7}/t_{0.3}$	6.01×10^{-3}
$t_{0.8}/t_{0.4}$	6.01×10^{-3}
Conventional $t_{1/2}$ method	
(does not include heat loss in formulation)	6.59×10^{-3}

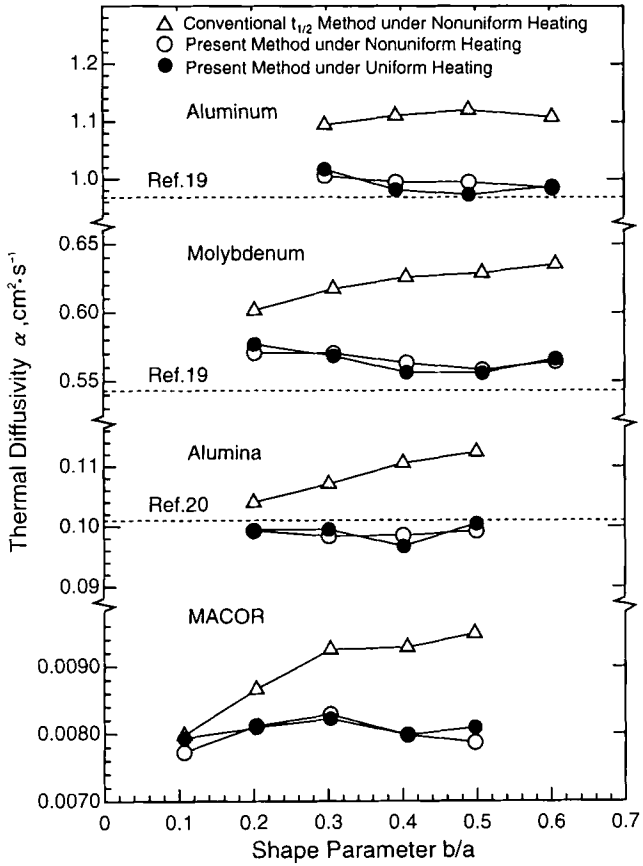

Fig. 11. The relationships between the thermal diffusivity and shape parameter for aluminum, molybdenum, alumina, and MACOR at 298.15 K. Open triangles represent the experimental values obtained by the conventional $t_{1/2}$ method under nonuniform heating conditions, open circles represent the experimental values obtained by the present modified curve-fitting method under nonuniform heating conditions and filled circles represent the experimental values obtained by the present modified curve-fitting method under uniform heating conditions. Dashed lines show the values reported in Refs. 19 and 20.

alumina and MACOR, the shape parameter dependence of the thermal diffusivities obtained by the conventional $t_{1/2}$ method results not only from the axially symmetric Gaussian nonuniform heating effect but also from heat loss. It should be emphasized that the distribution of energy absorbed by the specimen surface must be checked to confirm the degree of the

axially symmetric Gaussian nonuniform heating effect and heat loss effect simultaneously in the actual measurement For alumina and MACOR, thermal diffusivities obtained by the present modified curve-fitting method are independent of the shape parameter and energy distribution of the heating source, and the value for alumina agrees with the reported values [20] within 3%.

Figures 12 and 13 show the temperature dependence of the thermal diffusivity of molybdenum and MACOR, respectively. Open symbols represent the experimental values obtained by the present modified curve-fitting method under nonuniform conditions and filled symbols represent the experimental values obtained by the present modified curve-fitting method under uniform conditions. The dashed line shows the values reported in Ref. 19. The values obtained by the present modified curve-fitting method are independent of the shape parameter and agree with the reported values [19] within 3% under uniform and nonuniform heating conditions. In this experiment the maximum heat loss parameter L is 0.29 for MACOR at 1098.15 K. It is concluded that our present procedure sufficiently corrected for appreciable heat loss effect with an axially symmetric Gaussian nonuniform heating effect above room temperature.

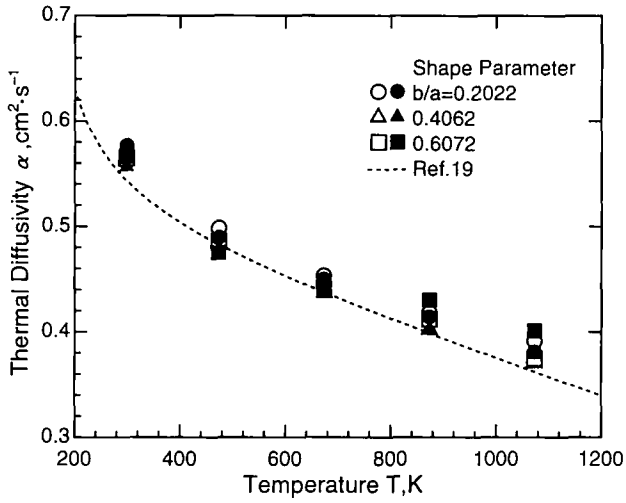

Fig. 12. Temperature dependence of the thermal diffusivity of molybdenum. Open symbols represent the experimental values obtained by the present modified curve-fitting method under nonuniform heating conditions and filled symbols represent the experimental values obtained by the present modified curve-fitting method under uniform heating conditions. The dashed line shows the values reported in Ref. 19.

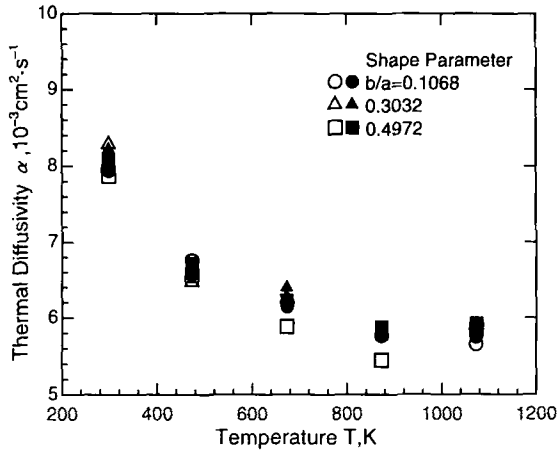

Fig. 13. Temperature dependence of the thermal diffusivity of MACOR. Open symbols represent the experimental values obtained by the present modified curve-fitting method under nonuniform heating conditions, and filled symbols represent the experimental values obtained by the present modified curve-fitting method under uniform conditions.

REFERENCES

1. W. J. Parker, R. J. Jenkins, C. P. Butler, and G. L. Abbot, *J. Appl. Phys.* **32**:1679 (1961).
2. F. Righini and A. Cezairliyan, *High Temp. High Press.* **15**:481 (1973).
3. T. Azumi and Y. Takahashi, *Rev. Sci. Instrum.* **52**:1411 (1981).
4. R. D. Cowan, *J. Appl. Phys.* **34**:926 (1963).
5. J. A. Cape and G. W. Lehman, *J. Appl. Phys.* **34**:1909 (1963).
6. R. C. Heckman, *J. Appl. Phys.* **44**:1455 (1973).
7. L. M. Clark III and R. E. Taylor, *J. Apply. Phys.* **46**:714 (1975).
8. J. B. Moser and O. L. Kruger, *J. Appl. Phys.* **38**:3215 (1967).
9. D. Shaw, L. A. Goldsmith, and A. Little, *Br. J. Appl. Phys. (J. Phys. D)* **2**:597 (1969).
10. H. M. James, *J. Appl. Phys.* **51**:4666 (1980).
11. P. S. Murti and C. K. Mathews, *J. Phys. D* **24**:2202 (1991).
12. D. Jossel, J. Warren, and A. Cezairliyan, *J. Appl. Phys.* **78**:6867 (1995).
13. D. A. Watt, *Br. J. Appl. Phys.* **17**:231 (1966).
14. J. A. McKay and J. T. Schriempf, *J. Appl. Phys.* **47**:1668 (1976).
15. T. Azumi, Y. Takahashi, and M. Kanno, in *Proceedings of the 2nd Japan Symposium on Thermophysical Properties*, Tokyo, (1981), p. 19 (in Japanese).
16. T. Baba, T. Arai, and A. Ono, in *Proceedings of the 7th Japan Symposium on Thermophysical Properties*, Tokyo, (1986), p. 235 (in Japanese).
17. T. Baba, M. Kobayashi, A. Ono, J. H. Hong, and M. M. Suliyanti, *Thermochim. Acta* **18**:329 (1993).

18. A. Cezairliyan, T. Baba, and R. Taylor, *Int. J. Thermophys.* **15**:317 (1994).
19. Y. S. Touloukian, R. W. Powell, C. Y. Ho, and M. C. Nicolaou, *Thermophysical Properties of Matter, Thermal Diffusivity*, TPRC Data Series (IFI Plenum, New York, 1973), Vol. 10.
20. M. Ogawa and T. Baba, in *Proceedings of the 15th Japan Symposium on Thermophysical Properties*, Tokyo, (1994), p. 85 (in Japanese).